

Trap-state Passivation of Titania Nanotubes by Electrochemical Doping for Enhanced Photoelectrochemical Performance

Lok-kun Tsui, Mikiko Saito, Takayuki Homma and Giovanni Zangari

Supporting Information

1. Raman spectroscopy

Raman spectra was acquired using a Renishaw inVia Raman microscope using a 488 nm laser and acquisition time of 10s per sample. XRD patterns were collected with a Panalytical X'Pert MPD using Cu $\kappa\alpha$ radiation. Raman spectra and XRD patterns were acquired before and after treatment with Li and H. All four detectable Raman peaks correspond to anatase TiO_2 ,^{1,2} and only anatase TiO_2 and the Ti substrate are detected with XRD. Detectable shifts were on the order of 0.5 cm^{-1} , well within the error resolution of the instrument. Similarly, no detectable shifts were found in the XRD patterns.

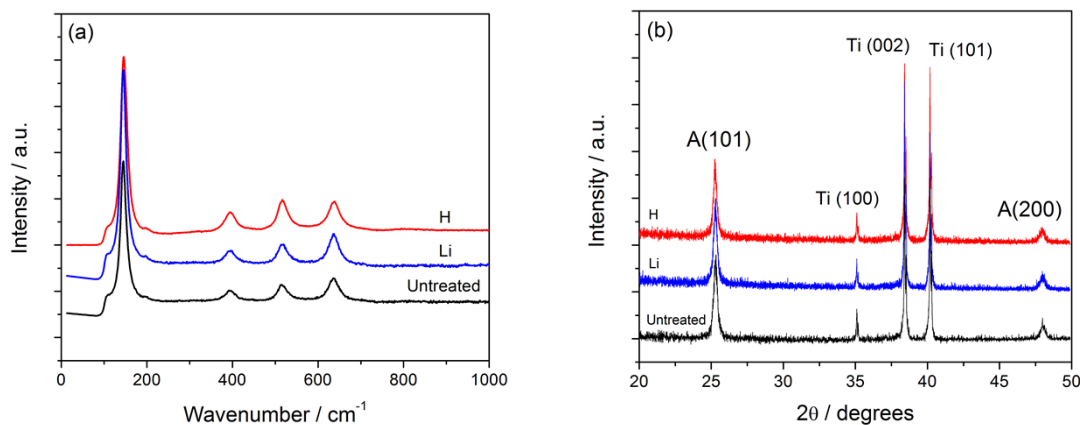


Figure S1. (a) Raman spectra and (b) XRD patterns of TiO_2 nanotubes before and after H / Li doping. A(h,k,l) and Ti(h,k,l) indicate reflections of anatase TiO_2 and the Ti substrate respectively.

2. FFT analysis of HR-TEM images

FFT analysis was carried out in a 5 nm x 5 nm square (Figure S2) using the Gatan Digital Micrograph software. The FFT patterns show a high degree of crystallinity in the TiO₂ nanotubes in the undoped case, but the more fuzzy spots of the TiO₂ NTs in the doped system points to a higher degree of disorder induced by the introduction of Li. The viewing directions were indexed to be (1, 2, 0) in the undoped case and (1, 0, 0) in the doped case. High index spots in both FFTs were selected and analyzed by Gaussian fitting with a linear baseline, giving a full width at half max of 0.492 nm⁻¹ and 0.616 nm⁻¹, respectively.

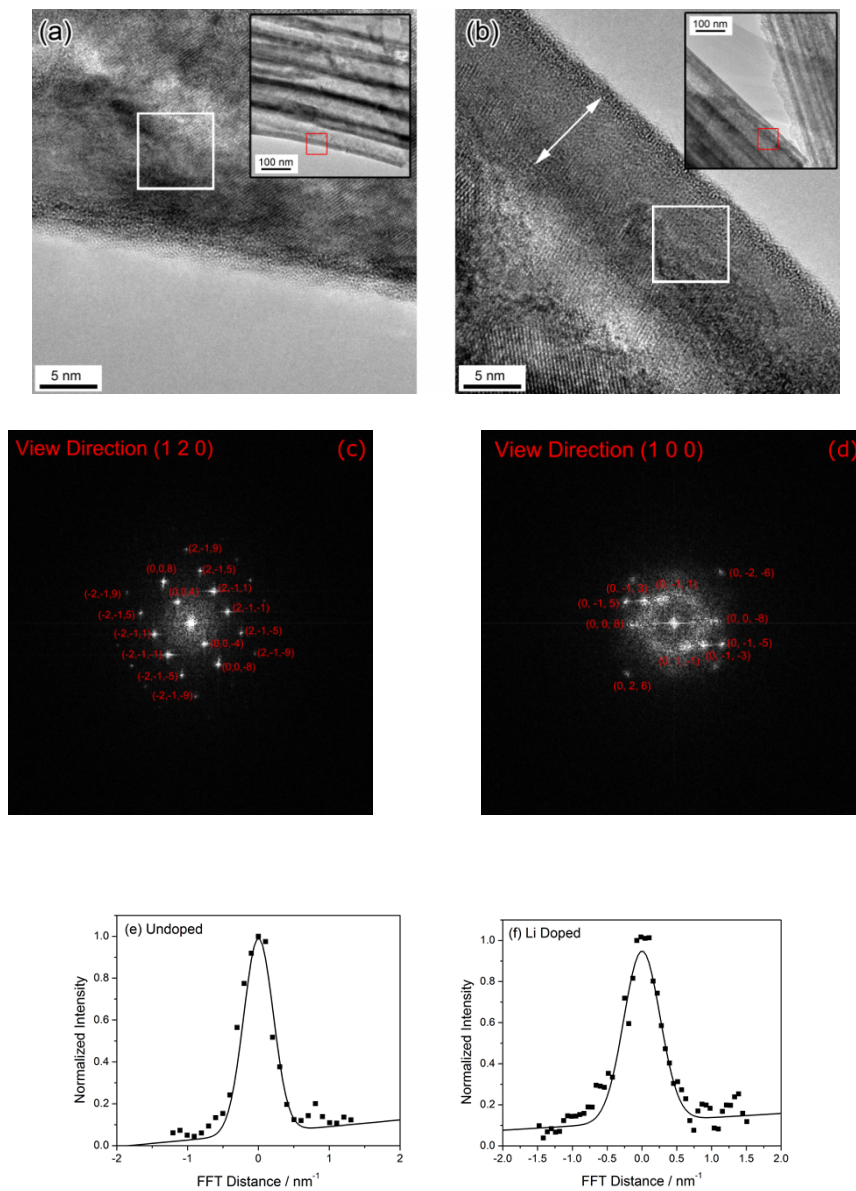


Figure S2. HR TEM images of (a) undoped and (b) Li doped TiO_2 nanotubes with white boxes in the main images to indicate the area where FFTs were taken from. The FFT patterns for (c) undoped and (d) Li doped TiO_2 nanotubes are shown below. (e) and (f) show the normalized intensity profiles for (2, -1, 5) and (0, -1, 5) peaks respectively for the undoped and doped TiO_2 NTs.

3. Calculation of space charge layer thickness

The space charge layer thickness is calculated from equation S1.³ Here ΔV is the potential difference with respect to the flatband potential, k is Boltzmann's constant, T is absolute temperature, e is the electron charge, ϵ is the dielectric constant (100),^{4,5} ϵ_0 is the permittivity of free space, and N_D is the density of donors (10^{20} cm^{-3} for TiO_2 NTs).²

$$W = \left(\frac{2\epsilon\epsilon_0}{eN_D} \right)^{\frac{1}{2}} \left(\Delta V - \frac{kT}{e} \right)^{\frac{1}{2}} \quad (\text{S1})$$

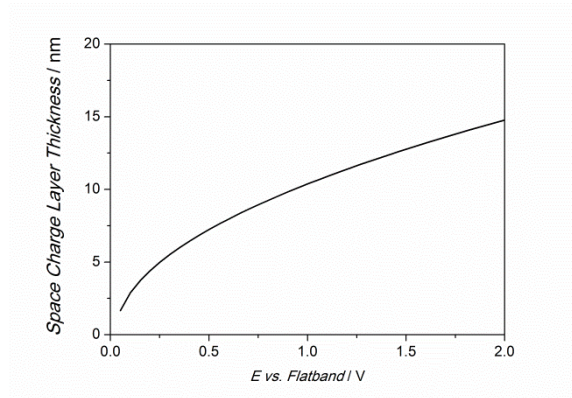


Figure S3. Space charge layer as a function of potential increases up to 15 nm under the application of 2 V vs. Flatband.

4. Effect of Increasing Lithium Loading

Because the density of trap states is orders of magnitude smaller than the amount of Li that is introduced by electrochemical doping, the addition of Li is found to have no effect on the photoelectrochemical performance.

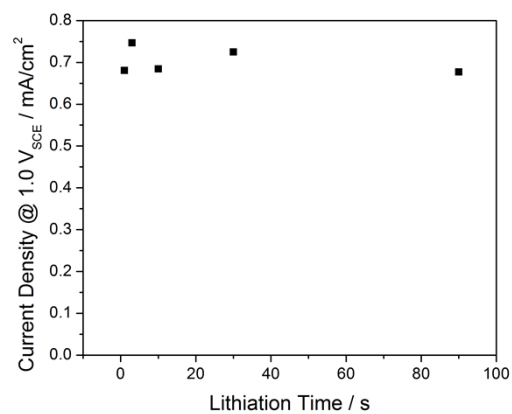


Figure S4. Effect of increasing reduction time on the photocurrent response of TiO₂ nanotubes.

References

1. S. Kang, J. Kim, H. Kim, and Y. Sung, *J. Indust. Eng. Chem.*, 2008, **14**, 52–59.
2. L. Tsui, T. Homma, and G. Zangari, *J. Phys. Chem. C*, 2013, **117**, 6979–6989.
3. G. K. Boschloo, *J. Electrochem. Soc.*, 1997, **144**, 1311.
4. S. A. Ali Yahia, L. Hamadou, A. Kadri, N. Benbrahim, and E. M. M. Sutter, *J. Electrochem. Soc.*, 2012, **159**, K83.
5. I. Hanzu, T. Djenizian, and P. Knauth, *J. Phys. Chem. C*, 2011, **115**, 5989–5996.